I&EC research
Industrial & Engineering Chemistry Research

Article

Cite This: Ind. Eng. Chem. Res. 2018, 57, 9693−9706

pubs.acs.org/IECR

SAFT-VR Mie: Application to Phase Equilibria of Alcohols in Mixtures with *n*-Alkanes and Water

Jamie T. Cripwell, Sonja A. M. Smith, Cara E. Schwarz, and Andries J. Burger*

Department of Process Engineering, Stellenbosch University, Private Bag X1, Matieland, 7602, South Africa

ABSTRACT: This work expands the scope of the SAFT-VR Mie framework by considering its application and that of its polar variant (SAFT-VR Mie-GV) to real phase behavior in alcohol/*n*-alkane and alcohol/water systems. This requires supplementing existing parameters for alcohols with parameter sets for all primary and secondary alcohols in the C_1-C_5 range. Parameter degeneracy is overcome using a novel variation of the discretized regression approach, by considering the average absolute deviations (AADs) for the mixture VLE resulting from each regressed parameter set in the discretized $\varepsilon^{AB}/k-n_p$ space. The resulting parameter sets exhibit excellent predictions for the alcohol/*n*-alkane and alcohol/water systems. The comparable results of the polar and nonpolar variants suggest that an explicit polar term is not necessary to describe the phase behavior of alcohols in the considered mixtures. The choice of association scheme is more significant, with the 2C scheme yielding excellent predictions for alcohols in mixtures with both alkanes and water.

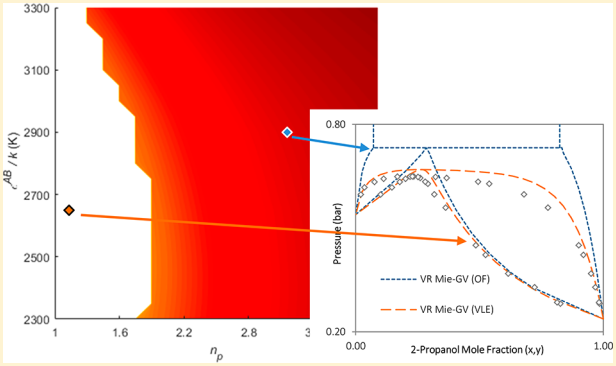

1. INTRODUCTION

Intermolecular association and its profound influence on macroscopic fluid properties were at the heart of the development of Wertheim's first-order thermodynamic perturbation theory (TPT1)[1−4] and, subsequently, the statistical associating fluid theory (SAFT).[5,6] The resulting network of hydrogen bonds characterize the thermodynamic behavior of many industrially relevant organic components, most notably alcohols. Primary and secondary alcohols are common products in petrochemical streams, fermentation broths, and pharmaceutical products,[7] which all require purification—traditionally, by means of distillation. This prevalence, and the economic significance of these industries, provide ample motivation for prioritizing the accurate description of these components and their mixtures in the development of thermodynamic models.

Contemporary models such as SAFT have their roots in fundamental disciplines of physics and chemistry, including statistical mechanics and molecular perturbation theory. As such, these models are thoroughly vetted using molecular simulations data to isolate theoretical inconsistencies before being applied to real fluids, where their true practical value lies. SAFT for Mie potentials of variable range, more commonly referred to as SAFT-VR Mie,[8−10] is a SAFT variant more deeply entrenched in these fundamental disciplines. The model incorporates the variable Mie potential (eq 1), rather than the more simplified square-well or Lennard-Jones potentials, to describe the intermolecular forces of the reference fluid, and considers a higher-order expansion than its contemporaries.[10]

$$u^{\mathrm{Mie}}(r) = \varepsilon\left[\frac{\lambda_r}{\lambda_r-\lambda_a}\left(\frac{\lambda_r}{\lambda_a}\right)^{\lambda_a/(\lambda_r-\lambda_a)}\right]\left[\left(\frac{\sigma}{r}\right)^{\lambda_r}-\left(\frac{\sigma}{r}\right)^{\lambda_a}\right] \quad (1)$$

This higher-order treatment yields excellent results when the model is applied to molecular simulation results, exhibiting marked improvement over previous iterations. Despite these excellent results, however, there has been limited application of SAFT-VR Mie to real fluids and their mixtures. Most published applications have been restricted to the *n*-alkane homologous series,[10,11] short chain ($\leq C_4$) primary alcohols,[10,12] water,[10,12] and carbon dioxide.[10,11] Indeed, subsequent development of the model has focused on implementing the third-order perturbation theory in a group-contribution (GC) approach (so-called SAFT-γ Mie[13,14]), rather than augmenting the progress made with SAFT-VR Mie.

The rationale for moving from SAFT-VR Mie to SAFT-γ Mie follows the traditional argument for GC approaches: the promise of a predictive model without the need for experimental data. There is still much debate as to whether GC approaches can ever truly achieve this level of accuracy, however, and SAFT-γ Mie results to date[13−16] suggest that much work still must be done to achieve this lofty goal. In light of these results, the modeling of industrially important mixtures remains the responsibility of traditionally parametrized models. The level of accuracy displayed by SAFT-

Received: March 9, 2018
Revised: June 26, 2018
Accepted: June 29, 2018
Published: June 29, 2018

DOI: 10.1021/acs.iecr.8b01042
Ind. Eng. Chem. Res. 2018, 57, 9693−9706

VR Mie suggests that the model is well-suited to this role, but its limited application raises questions regarding the wider application of the model.

In this work, we aim to address these questions by broadening the scope of SAFT-VR Mie to consider the full isomeric range of linear alcohols from C_1 to C_5. In this way, we further the analysis of mixture behavior for those components where parameter sets have been previously regressed, while augmenting that collection with parameter sets for the missing primary and secondary alcohols. The focus here is the accurate prediction of mixture phase behavior, considering linear alcohols in mixtures with nonassociating species (viz. *n*-alkanes), as well as aqueous mixtures.

2. THEORY

2.1. Parametrization. Similar to many of its contemporaries, SAFT-VR Mie is most frequently presented in the form of a residual Helmholtz energy expansion:

$$\frac{A^{r}}{NkT} = \frac{A^{seg}}{NkT} + \frac{A^{disp}}{NkT} + \frac{A^{chain}}{NkT} + \frac{A^{assoc}}{NkT} \tag{2}$$

The full model development is detailed in the original work of Lafitte and co-workers[10]—for the purposes of this work, we need only highlight the parameter set required for regression. The monomer and chain terms make use of the traditional, regressed segment diameter (σ), segment number (m), and dispersion energy (ε/k) parameters, but the use of the Mie intermolecular potential introduces two further parameters in the terms of eq 2. The attractive and repulsive range parameters (λ_a and λ_r, respectively) are responsible for the curvature of the potential function, and are cited as the reason SAFT-VR Mie yields accurate predictions for second-derivative properties.[8,9] Only the repulsive range is fitted to experimental data, however, with the attractive range fixed to a value of 6, corresponding to the range of the attractive London dispersion force.[10]

The association contribution in SAFT-VR Mie is defined using the same hard-sphere radial distribution function as its contemporaries, but is parametrized slightly differently. Later work[12] considered employing a Mie radial distribution function in the association term, but the degree of improvement in evidence does not seem to warrant the associated increase in computational intensity. The difference in parametrization approaches stems from the work of Jackson et al.[17] and is a result of the implicit temperature dependence introduced to the definition of association volume (κ^{AB}) through the use of the temperature-dependent segment diameter (d). Instead of regressing κ^{AB}, this quantity is redefined in terms of the range of association (r_c^{AB}) and the distance between the associating site and its corresponding segment center (r_d^{AB}), as per eq 3.

$$\kappa^{AB} = \frac{4\pi d^2}{72(r_d^{AB})^2\sigma^3}\left\{\ln\left(\frac{r_c^{AB} + 2r_d^{AB}}{d}\right)[6(r_c^{AB})^3 + 18(r_c^{AB})^2 r_d^{AB} - 24(r_d^{AB})^3] + (r_c^{AB} + 2r_d^{AB} - d)[22(r_d^{AB})^2 - 5r_c^{AB}r_d^{AB} - 7r_d^{AB} - 8(r_c^{AB})^2 + r_c^{AB}d + d^2]\right\} \tag{3}$$

The former (r_c^{AB}) replaces the association volume as the regressed parameter, while the latter is fixed to a value of 0.4σ (ref 18) and constrains the bonding geometry to verified ranges. Thus, SAFT-VR Mie requires a total of six parameters (four nonassociating parameters plus r_c^{AB} and the association energy parameter, ε^{AB}/k), fit to experimental data, for the description of real associating fluids and their mixtures.

When considering associating components such as alcohols, it is not only the parameter set, but also the selection of an *appropriate* association scheme that dictates prediction quality. This is a point that is often overlooked, with different association schemes tested in the pursuit of a better fit without due consideration of the physical appropriateness of these schemes for the components to which they are being applied. Physically speaking, the hydroxyl functional group comprises two proton acceptors and a proton donor, as indicated in Table 1, where the association schemes of interest to this work are presented.

Table 1. Hydroxyl Group Structure and Active Site Groupings of Different Association Schemes

Functional Group/Species	Association Scheme	Site Representation
Alcohols	3B	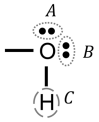
	2B	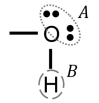
	2C	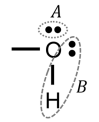

The hydroxyl group structure traditionally leads to two different treatments of alcohols, according to the original association schemes of Huang and Radosz.[6] Assigning the 3B scheme applies a more rigorous treatment, considering the possibility of hydrogen bonding at all three sites. However, this rigorous treatment is difficult to justify for alcohols larger than methanol, given the physical limitations of steric hindrance in longer chains. Therefore, the use of the 2B scheme offers a better approximation of these steric limitations by combining the lone electron pairs into a single proton acceptor site. A similar rationale was used in the development of the recently proposed the 2C scheme,[7] where the proton donor and one proton acceptor are combined to form a bipolar site, in addition to the remaining proton acceptor site. The consideration of a bipolar site is not new to the SAFT framework (as bipolar sites characterize the 1A scheme assigned to acids[6]), but the novel application of the bipolar site to alcohols[7] produced superior results for aqueous mixtures of primary alcohols in the sPC-SAFT framework. Whether these improvements extend to SAFT-VR Mie has yet to be tested.

2.2. The Question of Polarity. The aforementioned emphasis on physically representative parameter sets raises a question that is still to be definitively answered in the SAFT-modeling of alcohols, i.e., whether there is a need for an explicit polar term. Alcohols have a functional group average dipole moment of ~1.7 D.[19] While this is not as significant as that for ketones (ca. 2.7 D[20]), it is higher than that for ethers (ca. 1.1 D[19]) for which accurate model predictions have been

DOI: 10.1021/acs.iecr.8b01042
Ind. Eng. Chem. Res. 2018, 57, 9693−9706

shown to be predicated on the inclusion of an explicit polar term.[21−23] Based on this simple analysis, one could conclude that an explicit polar term is indeed necessary, but it is the self-associating nature of alcohols (not found in ketones and ethers) that makes the question harder to answer. Hydrogen bonds are of the order of 10−100 kJ/mol while the strong dipolar forces present in functional groups such as ketones are only in the 2−8 kJ/mol range.[24] Thus, while these strong dipolar forces do exist between alcohol molecules, the effects of association are much stronger and have a tendency to dictate the thermodynamic behavior of these components. It is for this reason that the "correct" fundamental treatment of these components remains uncertain.

The works of Al-Saifi et al.[25] and de Villiers et al.[26,27] demonstrate that the incorporation of a polar term yields improved predictions of VLE and LLE in alcohol-containing systems using PC- and sPC-SAFT, respectively. More recently, Fouad et al.[28] demonstrated that a polar term is *required* for the accurate description of infinite dilution activity coefficients and monomer fractions. However, the findings of these select few studies are in contrast to the majority of SAFT studies, where *sufficiently* accurate results are obtained for alcohols considering association alone. A hurdle to the more widespread adoption of an explicit polar treatment is the lack of consensus on the choice of polar term. Al-Saifi et al.[25] compared those of Jog and Chapman (JC),[21,29] Gross and Vrabec (GV),[22] and Karakatsani et al.,[30,31] concluding that the performance of the JC term was marginally superior, but that its parametrization was made difficult by the prominence of broad minima in the objective function. De Villiers et al.[26,27] concluded that there was little difference between the JC and GV terms if both terms were treated with a variable polar parameter. In the context of the work presented here, this last point can be addressed using the conclusions drawn from our recent work[23] on polar, nonassociating components, where the compatibility of the GV polar term with the SAFT-VR Mie framework was demonstrated. The modular nature of the SAFT framework facilitates the seamless addition of the GV polar term to the residual Helmholtz energy expansion of eq 2, and the reader is referred to our previous work[23] and the original work of Gross and Vrabec[22] for a more-detailed discussion of the working equations. Significantly, the inclusion of an explicit polar term introduces an additional parameter (n_p, which represents the number of polar segments), bringing the total number of parameters that require fitting to 7 for the polar SAFT-VR Mie-GV model.

In our current work, we endeavored to provide fresh insight into whether a polar term is necessary for the accurate thermodynamic description of alcohols. Thus, in addition to supplementing the existing SAFT-VR Mie parameter pool for alcohols, we will determine SAFT-VR Mie-GV parameters for these same alcohols and analyze the balance of dipolar and association effects in the SAFT-VR Mie framework for the first time.

3. REGRESSION

3.1. Property Choice. In order to achieve our aim of supplementing the SAFT-VR Mie parameter sets already determined by Lafitte et al.,[10] it would be prudent to follow the same regression strategy as was used in that work. Lafitte et al. used an objective function considering the sums of residuals in the saturated liquid density (ρ^{sat}) and vapor pressure (P^{sat}), as well as the density (ρ^{liq}) and ultrasonic speed (u^{liq}) of the condensed liquid. These properties were weighted according to a 4:4:1:1 ratio, with experimental data taken from the NIST database.[32] In this work, we make use of a similarly weighted objective function, using the DIPPR database[19] for the saturation properties. Experimental speed of sound data was sourced from the literature and listed in Table 2; the compressed liquid density is omitted from our regression function. This standard regression procedure (SRP), using pure component property data alone, is used for regression of the nonpolar SAFT-VR Mie parameter sets.

Table 2. Sources of Pure-Component Speed-of-Sound Data

component	property specification	range	reference
		Alcohols	
methanol	isothermal	303 K: 0.1−275 MPa	33
ethanol	isothermal	273 K: 0.1−30 MPa	34
		313 K: 0.1−30 MPa	34
		353 K: 0.1−30 MPa	34
1-propanol	isobaric	0.10 MPa: 293−318 K	35
2-propanol	isobaric	0.101 MPa: 288−308 K	36
	isothermal	273 K: 0.1−30 MPa	37
		333 K: 0.1−30 MPa	37
1-butanol	isothermal	273 K: 0.1−96 MPa	38
		303 K: 0.1−96 MPa	38
		323 K: 0.1−96 MPa	38
2-butanol	isobaric	0.101 MPa: 298−323 K	39
	isothermal	273 K: 0.1−30 MPa	37
		333 K: 0.1−30 MPa	37
1-pentanol	isothermal	303 K: 0.1−100 MPa	40
2-pentanol			
3-pentanol	isothermal	303 K: 0.1−100 MPa	41
		333 K: 0.1−100 MPa	41
		363 K: 0.1−100 MPa	41

In the case of the polar SAFT-VR Mie-GV parameter sets, it is necessary to include mixture data to yield a nonzero polar contribution.[23] This mixture data (MD) approach was originally proposed in the SAFT framework by Dominik et al.,[42] who advocated for the inclusion of ester/*n*-alkane VLE data in the objective function to differentiate between the contributions of the polar and dispersion terms. This approach has been more widely adopted in the recent SAFT literature, yielding highly accurate parameter sets in the PC-SAFT,[28,42,43] sPC-SAFT,[26,27,44] GC-SAFT,[45] and even the SAFT-γ Mie approach.[13,14,16] The approach has even evolved somewhat, considering different types of mixture data and distinguishing between different contributions. Fouad et al.[28,43] incorporated infinite dilution activity coefficient data for the associating component in a linear alkane to approximate the dispersion energy parameter more accurately, relative to the association energy. Solubility data[14,16] and excess enthalpies[15] have been used in the SAFT-γ Mie approach to determine cross-interaction parameters. In this work, we include binary VLE data of the relevant alcohol with an *n*-alkane, with a decreased

DOI: 10.1021/acs.iecr.8b01042
Ind. Eng. Chem. Res. 2018, 57, 9693−9706

regression weight (viz. P^{sat}:ρ^{sat}:u^{liq}:VLE is 5:4:1:0.5). This emphasizes the importance of accurate pure-component property predictions, while accounting for the unlike interactions manifested in the mixture data.

3.2. Challenges and Alternatives. In the context of SAFT modeling, the most prevalent regression problem is parameter degeneracy, where parameter values are pushed to physically meaningless or nonsensical values. This problem is exacerbated as the dimensionality of the parameter space increases with the number of fitted parameters, with common prevalence when four or more parameters require fitting. The problem has been reported in the parametrization of polar components in (s)PC-SAFT[22,42,44] and associating components in SAFT-VR Mie,[11] where four and six parameters require fitting, respectively. This parameter degeneracy is typically a result of the mathematical rigor of the numerical methods employed to locate the minimum of a very "flat" objective function—one which only considers pure-component properties in the SRP approach. This "flatness" indicates an insensitivity of the objective function to changes in any given parameter value, or equivalently, an excess of parameter sets able to predict the considered pure-component properties within an acceptable tolerance.

The general approach to combatting parameter degeneracy is increasing the prominence of the minimum in the objective function. Considering mixture data in the MD approach requires that regressed parameters need to accurately account for the like−unlike interactions, which are not present in the pure component. This essentially concentrates the range of parameter sets that satisfy the minimization criterion. An alternate approach is to reduce the dimensionality of the parameter space (or equivalently, the number of fitted parameters) by fixing the values of certain parameters—akin to fixing the value of λ_a to 6 in SAFT-VR Mie. As highlighted by this example, however, this fixing procedure cannot be done arbitrarily and must have a sound physical basis. The parameters of interest can be fixed to constant values, or fixed by statistically relevant correlations. This approach is particularly common when employing an explicit polar term. The original formulation of the GV polar term[22] considered a fixed n_p value of 1, corresponding to a single dipolar functional group for ketones, esters, and ethers. Works using the JC polar term frequently fix the product $x_p m$ to a constant value for different homologous series[21,46] while, in our own research, we have proposed the use of homologous group specific correlations,[27,44] depending on molar mass, to fix the values of n_p and x_p when using the GV and JC polar terms, respectively. This fixed polar parameter (FPP) approach[23] has already been implemented with great success for SAFT-VR Mie-GV considering polar, nonassociating components.

While fixing the value of the polar parameter in the regression procedure has proven successful, similar attempts at fixing the value of the association parameters have yielded parameter sets with relatively poor predictive capacity,[47,48] especially for mixtures. This is directly related to the order of magnitude difference between association and dipolar effects, and explains the sensitivity of the objective function (and thus accurate description of thermodynamic behavior) to the magnitude of the association parameters. However, while the assumption of constant values for association parameters has been shown to be oversimplified, the plethora of published parameter sets does demonstrate an expected range of parameter values. This is particularly true of the energy parameters that can be compared to experimental data[49] to gauge their physical realism. While knowledge of such a range can be used to set upper and lower bounds on parameter values during regression, it does not guarantee that a unique solution will be found.

Clark et al.[50] made clever use of these expected ranges by using a gridlike approach to parameter regression. This is achieved by considering discrete intervals between the bounds for two different parameters (specifically, ε/k and ε^{AB}/k) and regressing the remaining parameters for each considered pair. In this way, $m \times n$ matrices of objective function results and fitted parameters are produced for the m and n discrete values considered for the respective parameters. More significantly, however, these matrices allow for visualization of the parameter space and provide some intuition regarding the behavior around the minimum. This has allowed for a more-heuristic approach, with the parameters chosen by considering an acceptable error threshold for the objective function minimization, and then applying fundamental understanding of parameter values to select the "optimal" parameter set in that range. This is frequently not the mathematical minimum, but it does relax the rigor of a strict numerical minimization, which leads to parameter degeneracy.

This discretized regression approach has started to gain some traction, with many authors subsequently employing the technique.[11,51,52] Discretizing the dispersion and association energy parameters allows for distinction to be drawn between the relative contributions of the two intermolecular forces, although different combinations of parameters have since been used. Dos Ramos et al.[52] paired the range (λ) parameter with the segment diameter and segment number for the treatment of nonassociating components to investigate the effect of long-range interactions in the SAFT-VR[53,54] framework. Dufal et al.[11] considered several combinations of parameters in the SAFT-VR Mie set and took the application of the discretization approach one step further by incorporating the corresponding contour plots for the percentage absolute average deviations (%AADs) of pure-component properties not included in the objective function. This last point is particularly poignant, because it provides a basis for a new means of parameter set analysis in the SAFT framework.

3.3. Approach. Parameter regression for associating species necessitates the selection of an association scheme. As has already been stressed, physical considerations are emphasized in the current work rather than the best mathematical fit. To this end, we consider the 3B scheme for methanol alone, while the performance of the 2B and 2C schemes is compared for all alcohols.

In all cases, the objective function was minimized using a Levenberg−Marquardt algorithm, considering a least-squares objective function. However, the regression strategy and formulation of that objective function was largely dictated by the nature of the regression space for the nonpolar and polar SAFT-VR Mie models. For nonpolar SAFT-VR Mie, the SRP approach was employed using the objective function, as specified in the Property Choice section above. This approach was determined to be sufficient for the determination of parameter sets for all considered components and association schemes.

In the case of SAFT-VR Mie-GV, the SRP approach was found to be entirely inadequate for parameter fitting with the previously described parameter degeneracy in evidence in all cases. It was for this reason that the MD approach had to be

DOI: 10.1021/acs.iecr.8b01042
Ind. Eng. Chem. Res. 2018, 57, 9693−9706

Table 3. SAFT-VR Mie Parameters Regressed by the SRP Approach for Primary and Secondary Linear Alcohols from C_1 to C_5, as Well as Water[a]

	M_W (g mol^{-1})	σ (Å)	m	ε/k (K)	λ_r	ε^{AB}/k (K)	r_c^{AB}/σ	P^{sat}, %AAD[b]	ρ^{sat}, %AAD[b]	u^{liq}, %AAD[c]	H^{vap}, %AAD[b]
3B Scheme											
methanol	32.04	2.8985	2.2728	166.57	6.787	2521.48	0.3802	0.90	0.10	2.67	4.41
2B Scheme											
methanol	32.04	3.1208	1.7930	158.57	8.467	2754.06	0.4428	0.79	0.08	1.93	0.74
ethanol	46.07	3.4379	1.9548	206.62	10.635	2852.14	0.3980	0.29	0.07	1.07	1.47
1-propanol[d]	60.09	3.5612	2.3356	227.66	10.179	2746.20	0.3538	0.83	0.25	0.19	1.48
2-propanol	60.09	3.4405	2.5794	208.00	10.274	2690.76	0.3519	0.40	0.24	1.42	1.68
1-butanol[d]	74.12	3.7856	2.4377	278.92	11.660	2728.10	0.3245	0.70	0.63	3.49	1.48
2-butanol	74.12	3.6438	2.6900	250.14	11.163	2594.80	0.3164	0.38	0.29	1.57	1.91
1-pentanol	88.14	4.014	2.4568	308.76	12.633	2632.72	0.3411	0.28	0.17	1.06	1.63
2-pentanol	88.14	4.1195	2.2813	306.92	12.885	2843.36	0.3011	0.15	0.25	1.06	2.22
3-pentanol	88.14	4.1647	2.2035	335.96	14.881	2542.45	0.3285	0.92	0.20	1.51	2.50
averages								**0.53**	**0.24**	**1.48**	**1.68**
2C Scheme											
methanol	32.04	3.2028	1.6626	173.76	8.965	2871.61	0.3992	0.77	0.09	1.74	1.67
ethanol	46.07	3.5592	1.7728	224.50	11.319	3018.05	0.3547	0.39	0.10	0.96	2.46
1-propanol	60.09	3.6008	2.2513	253.45	11.960	2794.88	0.3481	0.06	0.08	1.80	1.46
2-propanol	60.09	3.4662	2.5156	213.91	10.617	2845.76	0.3206	0.29	0.19	1.05	1.48
1-butanol	74.12	3.7704	2.4614	266.49	11.338	2910.05	0.3042	0.15	0.23	1.59	1.93
2-butanol	74.12	3.6422	2.6879	251.07	11.212	2743.47	0.2871	0.32	0.26	1.23	1.90
1-pentanol	88.14	4.0186	2.4451	311.17	12.741	2774.96	0.3103	0.22	0.14	1.01	1.61
2-pentanol	88.14	4.1216	2.2740	308.55	12.966	3001.89	0.2757	0.14	0.22	0.86	2.20
3-pentanol	88.14	4.2516	2.0902	354.83	15.748	2694.37	0.2969	0.95	0.19	1.33	2.48
averages								**0.37**	**0.17**	**1.29**	**1.91**
4C Scheme											
water	18.01	2.4539	1.7311	110.85	8.308	1991.07	0.5624	0.39	0.71	0.64	1.58

[a]Note: λ_a and r_c^{AB} fixed to values of 6 and 0.4σ, respectively. [b]%AADs with reference to appropriate DIPPR Correlations.[19] [c]%AADs in u^{liq} calculated with reference to data sets in Table 2. [d]Original parameter sets of Lafitte et al.[10]

considered for the polar model. However, this strategy was not successful in all cases, and for this reason, it was necessary to consider a similar approach to the discretized regression strategy of Clark et al.,[50] which will be discussed in the results that follow.

4. RESULTS

As has been emphasized throughout this work, our focus is the generation of practical parameter sets with high predictive capacity for application to real industrial mixtures of interest. To this end, we briefly consider the trends of the regressed parameter sets and their application to pure-component properties, before focusing on their predictive capacity considering phase behavior of both alcohol/*n*-alkane and alcohol/water mixtures.

4.1. Regressed Parameters and Trends. The regressed parameter sets for nonpolar SAFT-VR Mie are presented in Table 3. However, only the 1-propanol and 1-butanol parameter sets of Lafitte et al. are reproduced here, while those for methanol and ethanol have been refitted. The reason for doing so was that, upon application to mixture VLE data (which was not done by Lafitte et al.), the parameter sets for methanol and ethanol produced poor predictions with erroneous liquid splitting, as typified by the prediction for ethanol/*n*-heptane[55] in Figure 1. The parameters for water were similarly refitted to provide better predictions of mixture behavior, although only pure-component data were used in regressing these parameters.

The regressed parameters follow typical behavior of SAFT-type models, with an increase in chain length resulting in larger values of σ, m, ε/k, and λ_r. The association parameters exhibit the opposite trend with molecular weight, however, with smaller effective magnitudes of association as the chain length increases. This is consistent with the role of steric hindrance limiting the degree of association in these longer chains. Comparing the 2B and 2C scheme parameter sets, with the exception of the segment number, the 2B scheme parameters are consistently smaller than their 2C scheme counterparts. The parameters of both schemes adhere to experimentally measured values for the association energy, however, with

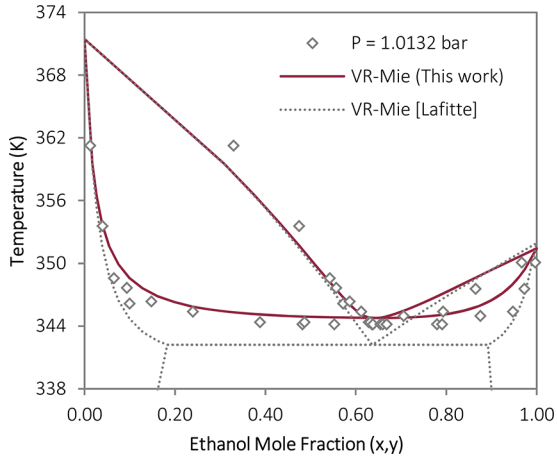

Figure 1. Comparison of prediction quality for ethanol parameter sets of Lafitte et al.[10] and this work, using VLE data for the ethanol/*n*-heptane system at 1.0132 bar.[55]

DOI: 10.1021/acs.iecr.8b01042
Ind. Eng. Chem. Res. 2018, 57, 9693−9706

Table 4. SAFT-VR Mie-GV Parameters Regressed by the MD Approach for Primary and Secondary Linear Alcohols from C_1 to C_5, as Well as Water[a]

	M_W (g mol^{-1})	σ (Å)	m	ε/k (K)	λ_r	ε^{AB}/k (K)	r_c^{AB}/σ	n_p	paired alkane[b]	P^{sat}, % AAD[c]	ρ^{sat}, % AAD[c]	u^{liq}, % AAD[d]	H^{vap}, % AAD[c]
3B Scheme													
methanol	32.04	2.9774	1.9975	163.63	9.940	2588.15	0.4202	0.2614	*n*-hexane[59]	1.88	0.19	2.34	3.49
2B Scheme													
methanol	32.04	3.1559	1.7195	169.76	9.327	2777.34	0.4502	0.1279	*n*-hexane[59]	0.83	0.07	1.73	1.18
ethanol	46.07	3.4462	1.9436	204.32	10.485	2857.92	0.3959	0.2764	*n*-heptane[55]	0.29	0.08	1.02	1.46
1-propanol[e]	60.09								*n*-heptane[60]				
2-propanol[e]	60.09								*n*-hexane[61]				
1-butanol[e]	74.12								*n*-heptane[62]				
2-butanol	74.12	3.6990	2.5839	241.04	10.62	2679.49	0.3063	1.5680	*n*-heptane[63]	0.46	0.34	0.98	1.83
1-pentanol	88.14	4.0621	2.3796	307.13	12.554	2661.86	0.3362	1.8315	*n*-heptane[64]	0.29	0.18	1.02	1.57
2-pentanol	88.14	4.1989	2.1683	306.19	12.793	2899.69	0.2929	2.1358	*n*-heptane[65]	0.19	0.27	0.94	2.02
3-pentanol	88.14	4.3882	1.9226	352.33	15.843	2620.99	0.3196	2.9158	*n*-heptane[66]	0.53	0.23	1.34	2.75
averages										**0.43**	**0.20**	**1.17**	**1.80**
2C Scheme													
methanol	32.04	3.3277	1.4774	188.61	10.296	2903.87	0.4073	0.4760	*n*-hexane[59]	0.73	0.06	1.58	3.98
ethanol	46.07	3.3978	2.0100	201.59	10.733	2815.52	0.3864	0.9106	*n*-heptane[55]	1.97	0.53	1.30	2.91
1-propanol	60.09	3.6280	2.2048	245.63	11.456	2855.32	0.3386	0.7454	*n*-heptane[60]	0.07	0.11	0.10	1.40
2-propanol	60.09	3.4795	2.4902	212.87	10.525	2865.19	0.3178	0.3016	*n*-hexane[61]	0.30	0.19	0.92	1.48
1-butanol[e]	74.12								*n*-heptane[62]				
2-butanol	74.12	3.7261	2.5296	244.94	10.855	2837.87	0.2766	1.9736	*n*-heptane[63]	0.38	0.30	1.00	1.76
1-pentanol	88.14	4.1003	2.3180	312.39	12.784	2821.07	0.3033	2.2526	*n*-heptane[64]	0.25	0.16	0.98	1.50
2-pentanol	88.14	4.2047	2.1563	309.65	13.001	3048.35	0.2702	2.1507	*n*-heptane[65]	0.14	0.24	0.95	2.07
3-pentanol	88.14	4.4353	1.8689	366.06	16.451	2754.78	0.2957	2.3909	*n*-heptane[66]	0.52	0.26	1.24	3.03
averages										**0.55**	**0.23**	**1.01**	**2.27**
4C Scheme													
water[f]	18.01	2.4539	1.7311	110.85	8.308	1991.07	0.5624	0		0.39	0.71	0.64	1.58

[a]Note: λ_a and r_c^{AB} fixed to values of 6 and 0.4σ, respectively [b]The source of the paired alkane data in indicated beside the name of the alkane. [c]% AADs with reference to appropriate DIPPR Correlations.[19] [d]%AADs in u^{liq} calculated with reference to data sets in Table 2. [e]Unable to generate unique polar parameter set resulting from parameter degeneracy. [f]Water treated as a nonpolar component with identical parameters to nonpolar model.

ε^{AB}/k falling in the 2526−3007 K range reported by Kontogeorgis et al.[56] Using similar physical arguments, the association energies for methanol (3B scheme) and water (4C Scheme) are comparable to their experimentally measured values of 2630 K[49] and 1813 K,[57] respectively.

The %AADs reported in Table 3 show excellent predictions of saturation properties (<1%) and speed-of-sound data (<4%). However, with these properties having been included in the objective function, the %AADs for heat of vaporization provide more context on the predictive capacity of the parameter sets; moreover, the sensitivity of the property to association effects[7,9,58] make it a good test of model performance for alcohols and water. In this context, the average values of 1.80% and 1.94% for 2B and 2C schemes, respectively, demonstrate a high level of prediction accuracy. The results for the alcohols are comparable with those previously seen in the SAFT-VR Mie framework,[10] while the %AAD for water is ca. 60% smaller than similar values reported using sPC-SAFT,[26] with no reported value available for comparison in SAFT-VR Mie.

The regressed parameter sets for polar SAFT-VR Mie-GV are presented in Table 4, the most notable feature of which is the missing parameter sets for 1-propanol, 2-propanol and 1-butanol using the 2B scheme, and for 1-butanol using the 2C scheme. This was a result of the aforementioned parameter degeneracy, but will be more thoroughly discussed in the Discretized Regression section below.

The regressed parameters follow the same trends as were evident for the nonpolar SAFT-VR Mie model, with the longer-chain alcohols exhibiting larger values of σ, m, ε/k, and λ_r, and smaller r_c^{AB} values. The association energies display a less-definite trend with molecular weight, seeming to remain constant independent of molecular size within each association scheme. The most notable parameter trend is in the regressed

DOI: 10.1021/acs.iecr.8b01042
Ind. Eng. Chem. Res. 2018, 57, 9693−9706

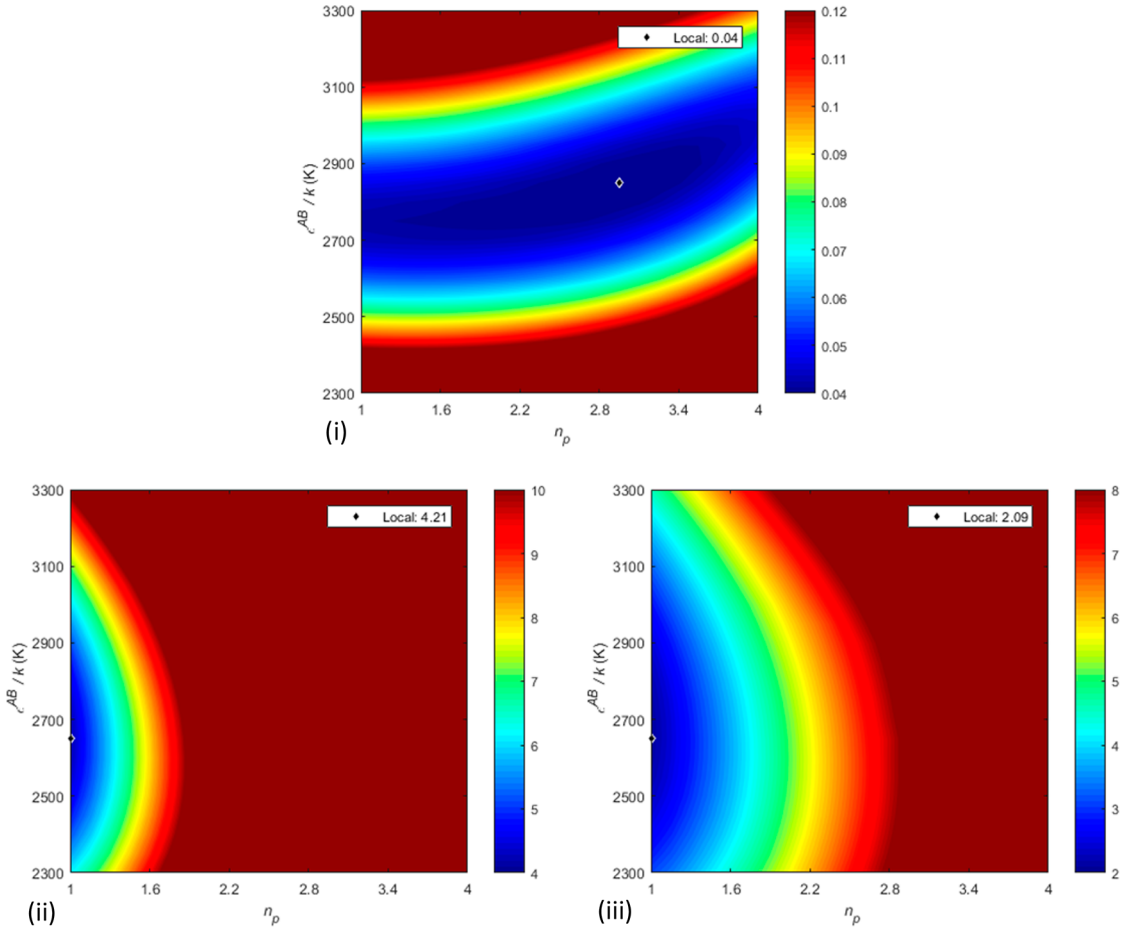

Figure 2. Contour plots for discretized regression of 2-propanol (2B) parameters: (i) objective function, (ii) AADy, and (iii) %AADP, using data for the 2-propanol/*n*-hexane system at 323.15 K.[61]

Table 5. SAFT-VR Mie-GV Parameters Determined by Discretized Regression, Considering Parameters Corresponding to the OF and AAD (VLE) Minima[a]

	M_W (g mol^{-1})	σ (Å)	m	ε/k (K)	λ_r	ε^{AB}/k (K)	r_c^{AB}/σ	n_p	P^{sat}, % AAD[b]	ρ^{sat}, % AAD[b]	u^{liq}, % AAD[c]	H^{vap}, % AAD[b]
1-Propanol (2B Scheme)												
OF min	60.09	3.8621	1.8962	221.263	9.9271	2900	0.3149	2.80	0.28	0.34	1.57	1.00
AAD min	60.09	3.4386	2.5498	233.725	11.5728	2500	0.4129	1.00	0.12	0.50	8.23	1.50
2-Propanol (2B Scheme)												
OF min	60.09	3.7463	2.0783	203.184	9.9240	2850	0.3018	2.95	0.50	0.40	1.47	0.91
AAD min	60.09	3.4121	2.6339	200.664	10.1352	2650	0.3590	1.00	0.39	0.34	1.95	1.56
1-Butanol (2B Scheme)												
OF min	74.12	4.1011	1.9802	270.516	11.3639	3000	0.2901	3.85	0.34	0.37	1.44	1.04
AAD min	74.12	4.3464	1.6969	300.779	10.6584	3300	0.2666	1.15	0.82	1.19	3.48	1.59
1-Butanol (2C Scheme)												
OF min	74.12	4.1148	1.9584	277.726	11.8150	3150	0.2668	4.00	0.25	0.32	1.25	0.92
AAD min	74.12	4.1077	1.9651	277.892	10.6689	3300	0.2615	1.45	0.51	0.67	3.29	1.61

[a]Note: λ_a and r_c^{AB} fixed to values of 6 and 0.4σ, respectively. [b]%AADs with reference to appropriate DIPPR Correlations.[19] [c]%AADs in u^{liq} calculated with reference to data sets in Table 2.

n_p values, which are <1 for the shorter-chain alcohols and increase as the chain gets longer. This same behavior was evident when the GV polar term was applied to alcohols in the sPC-SAFT framework.[26] The %AADs for the pure component properties are comparable to those of the nonpolar model, with marginally better representation of the speed-of-sound data as the only notable difference. With such similar performance in application to pure-component properties, application to mixture data is necessary to distinguish between model performance.

4.2. Discretized Regression. The discretized regression approach was used to determine parameter sets for those components affected by parameter degeneracy using the MD approach. The original discretization of ε/k and ε^{AB}/k was employed to distinguish between the dispersion and association effects on component behavior. Applying this

DOI: 10.1021/acs.iecr.8b01042
Ind. Eng. Chem. Res. 2018, 57, 9693−9706

approach to SAFT-VR Mie-GV parametrization, we chose to discretize the association energy and the number of polar segments (n_p). The rationale for this selection was 2-fold: first, it fixed the value of the polar parameter to a nonzero value, ensuring a nonzero polar contribution; and second, it allowed us to specifically investigate the relative influence of the polar term, compared to the stronger association effects.

Twenty discrete intervals in the ranges $\varepsilon^{AB}/k \in [2300\ \text{K}, 3300\ \text{K}]$ and $n_p \in [1,4]$ were selected; the ε^{AB}/k values encompass the range of experimentally measured enthalpies of association, while the n_p values correspond to the range of significant polar contributions that maintain physical realism. The remaining parameters were fitted using the same objective functions and weightings as were used for the SRP approach.

While the SRP approach was used in the objective function, the role of mixture data was incorporated by analyzing the average absolute deviations (AADs) in temperature/pressure and vapor composition for each parameter set. The work of Dufal et al.[11] gave impetus to the decision to consider these contour plots in addition to that for the objective function, as shown for 2-propanol in Figure 2. Analyzing the contours in Figure 2(i), it is clear that the objective function is relatively insensitive to the value of the polar parameter, with constant OF values for ca. $n_p \leq 3.4$. Indeed, the best mathematical fit for the objective function occurs at the combination $\varepsilon^{AB}/k = 2850$ K and $n_p = 2.95$, although similar results are obtainable in the full n_p range for $\varepsilon^{AB}/k \in [2700\ \text{K}, 3000\ \text{K}]$. These results are in stark contrast with the corresponding AADy and %AADP plots, which present a much more definite minimum combination of $\varepsilon^{AB}/k = 2650$ K and $n_p = 1$, as well as steeper gradients in the immediate space. The ramifications of this are only clear when one considers the predictions based on these parameter sets.

Table 5 contains two parameter sets for each of the missing alcohols in Table 4: the first is the parameter set corresponding to the mathematical minimum of the objective function (Figure 2(i)), while the other represents the best fit for experimental VLE data, or the minimum of Figures 2(ii) and 2(iii). Considering the %AADs in pure-component properties of the different parameter sets, the influence of the broad minimum becomes clear—despite significant differences in the magnitudes of the polar and associating parameters, both parameter sets yield comparable results for the prediction of pure-component properties. The only significant difference in shifting from the rigorous OF minimum to the more heuristic AAD minimum is in the prediction of the speed of sound for 1-propanol. However, this decreased accuracy in u coincides with improved predictions for the saturation properties—indeed, the same trend is evident for 2-propanol. This demonstrates the potential shortfalls of relying on mathematical rigor in regressing SAFT parameters.

This point is further emphasized when the same parameter sets are used for the prediction of mixture properties, as in Figure 3 for the prediction of VLE in the 1-propanol/n-heptane[60] binary mixture. The AAD minimum parameter set shows excellent agreement with the experimental data, while the OF minimum parameters falsely predict liquid splitting and offers poor prediction of the liquid composition in general. This was a common feature of the OF minimum parameter sets for the smaller alcohols, with the same trend evident for 2-propanol.

The difference in prediction quality suggests that a limiting balance between the association and polar contributions exists,

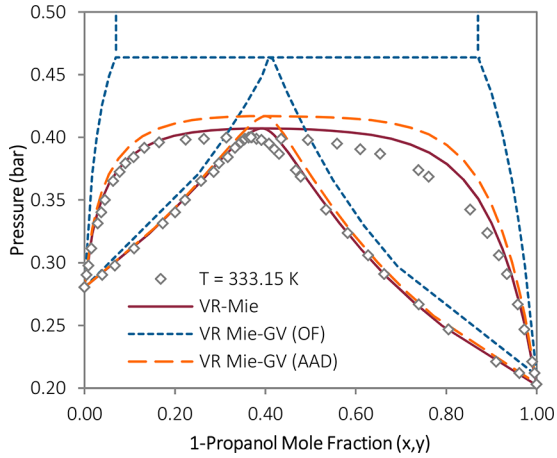

Figure 3. Comparison of prediction quality for 1-propanol parameter sets determined from the OF and AAD minima in the contour plots of Figure 2, using VLE data for the 1-propanol/n-heptane system at 333.15 K.[60]

beyond which erroneous liquid splitting behavior will be predicted. This motivated a widening of the scope of the discretized regression approach to test for liquid splitting tendencies in the discretized parameter sets to determine whether such a boundary exists. The result is a contour plot such as that presented for the 1-propanol/n-heptane system in Figure 4. The empty (white) space indicates the ε^{AB}/k–n_p

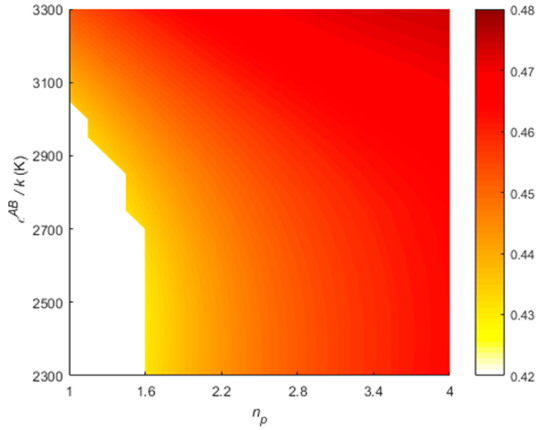

Figure 4. Contour plot of the predicted heteroazeotropic pressure (bar) in the 1-propanol/n-heptane system at 333.15 K.[60] Empty space indicates the absence of VLLE behavior.

combinations, which do not predict vapor–liquid–liquid equilibrium (VLLE) behavior, while the contours show the predicted heteroazeotropic pressure. Figure 4 demonstrates the limited range of viable parameter sets which accurately capture the macroscopic fluid behavior and confirms the behavior of the parameter sets displayed in Figure 3.

The results of this section clearly demonstrate the heuristic value of the discretized regression approach. The broad minimum resulting from an objective function that only considers pure component properties gives rise to a plethora of viable parameter sets, the mathematical minimum of which has no physical significance. Using the contour plots of Figures 2 and 4 allows us to introduce fundamental principles to determine the most appropriate parameter set by applying limits of acceptability to the objective function results. The

DOI: 10.1021/acs.iecr.8b01042
Ind. Eng. Chem. Res. 2018, 57, 9693–9706

Table 6. Average AAD Values Summarizing the Prediction Quality of SAFT-VR Mie and SAFT-VR Mie-GV Applied to Alcohol/*n*-Alkane and Alcohol/Water Systems

	Alcohol/*n*-Alkane Mixtures			Alcohol/Water Mixtures		
	Δy ($\times 10^2$)	ΔP (%)/ΔT(K)	No. of data sets	Δy ($\times 10^2$)	ΔP (%)/ΔT(K)	No. of data sets
SAFT-VR Mie						
SAFT-VR Mie (3B Scheme)	12.38	58.31%/10.36 K	3[a]	3.96	13.65%/2.84 K	2[b]
SAFT-VR Mie (2B Scheme)	1.50	3.45%/2.04 K	20[c]	4.82	16.48%/3.57 K	10[d]
SAFT-VR Mie (2C Scheme)	1.44	3.52%/1.35 K	20[c]	2.19	7.73%/1.63 K	10[d]
SAFT-VR Mie-GV						
SAFT-VR Mie-GV (3B Scheme)	4.02	11.65%/2.76 K	3[a]	4.23	23.1%/3.72 K	2[b]
SAFT-VR Mie-GV (2B Scheme)	1.35	2.66%/0.75 K	20[c]	5.31	18.82%/3.74 K	10[d]
SAFT-VR Mie-GV (2C Scheme)	1.01	3.19%/0.57 K	20[c]	2.48	10.09%/1.41 K	10[d]

[a]Data taken from refs 59, 67, and 68. [b]Data taken from refs 75 and 76. [c]Data taken from refs 55 and 59−74. [d]Data taken from refs 75−82.

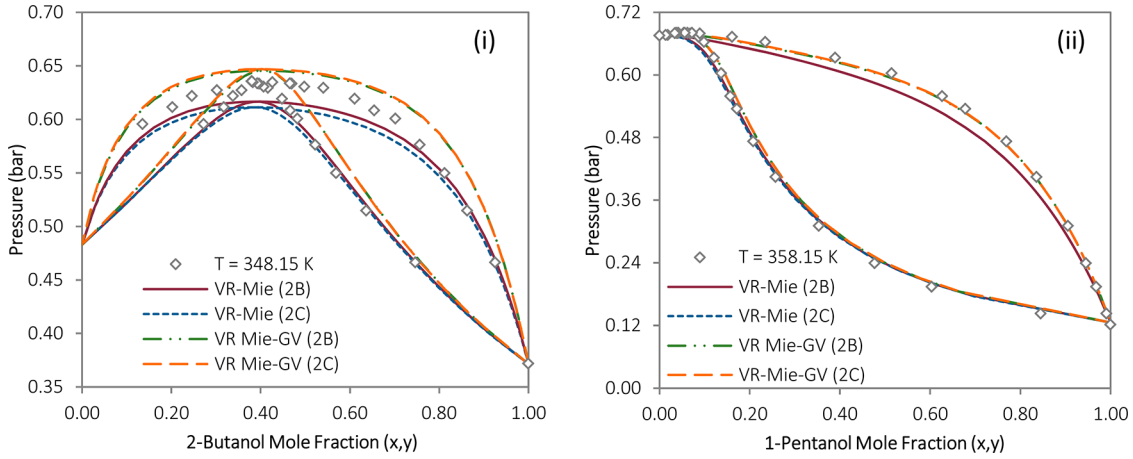

Figure 5. Comparison of polar and nonpolar SAFT-VR Mie parameter sets applied to alcohol/*n*-alkane mixtures: (i) 2-butanol/*n*-heptane at 348.15 K[63] and (ii) 1-pentanol/*n*-heptane at 358.15 K.[64]

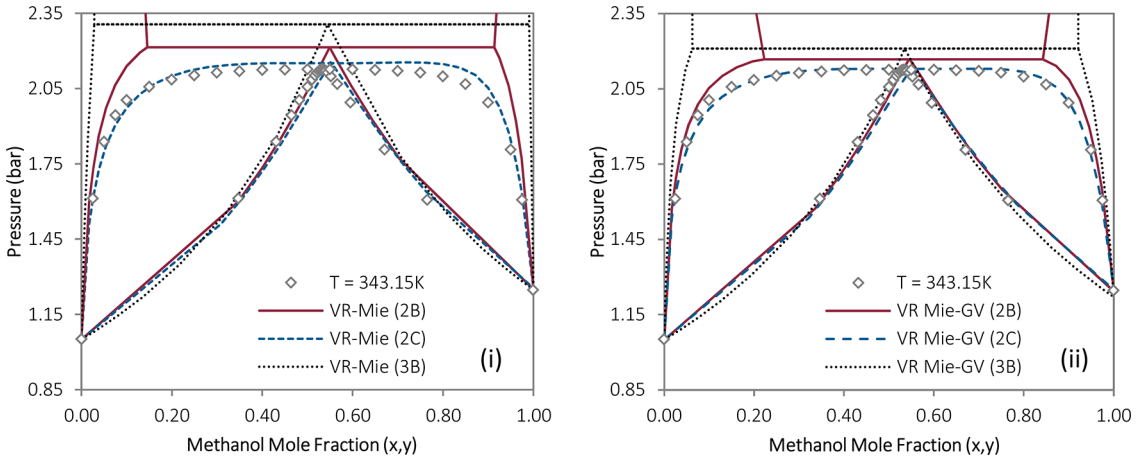

Figure 6. Comparison of predictions for methanol/*n*-hexane at 343.15 K,[59] using different association schemes: (i) nonpolar SAFT-VR Mie and (ii) SAFT-VR Mie-GV.

discretized regression approach opens the door to more fundamental analysis of regressed parameter sets—an aspect that we will try to explore in future work. In the context of this study, however, it has allowed for the determination of SAFT-VR Mie-GV parameter sets, which can be tested using real-mixture phase behavior in the section that follows.

4.3. Mixture VLE. The alcohol parameters of Tables 2, 3, and 4 were used to produce VLE predictions for alcohol/*n*-alkane and alcohol/water systems, the average AAD values for which are summarized in Table 6.

Considering the alcohol/*n*-alkane systems, the first comparison can be drawn between the performance of the polar and nonpolar models. Generally, there is slight improvement in the prediction quality of SAFT-VR Mie-GV, compared to its nonpolar counterpart. The more notable improvements are apparent in the temperature/pressure description in the larger alcohols (C_4 and C_5), as shown in Figure 5. The opposite was true for the smaller alcohols, as Figure 3 attests, with the polar model yielding poorer predictions than its nonpolar counterpart. These results suggest that the hydrogen bonding effects

DOI: 10.1021/acs.iecr.8b01042
Ind. Eng. Chem. Res. 2018, 57, 9693−9706

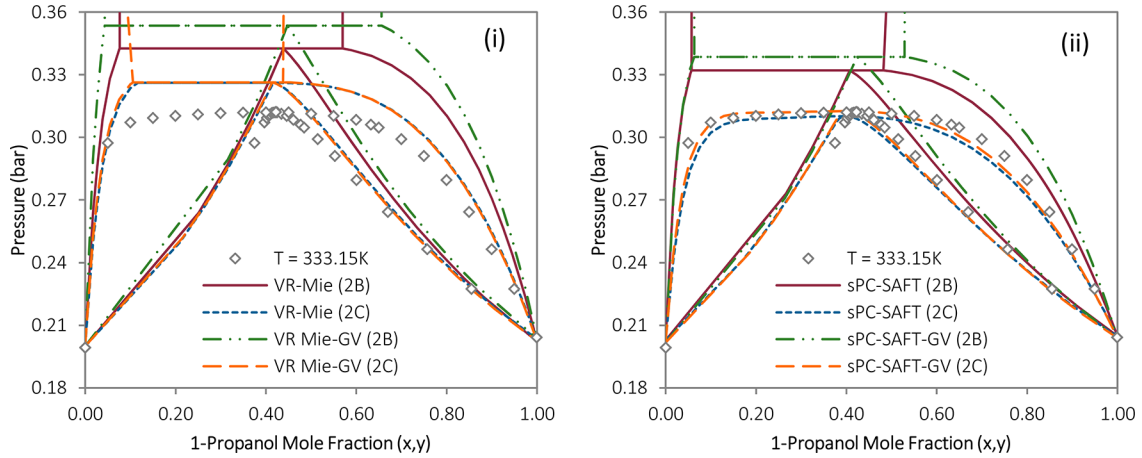

Figure 7. Comparison of predictions for polar and nonpolar models, considering the 2B and 2C schemes, applied to 1-propanol/water system at 333.15 K:[78] (i) SAFT-VR Mie and (ii) sPC-SAFT with literature parameters.[7,27,48]

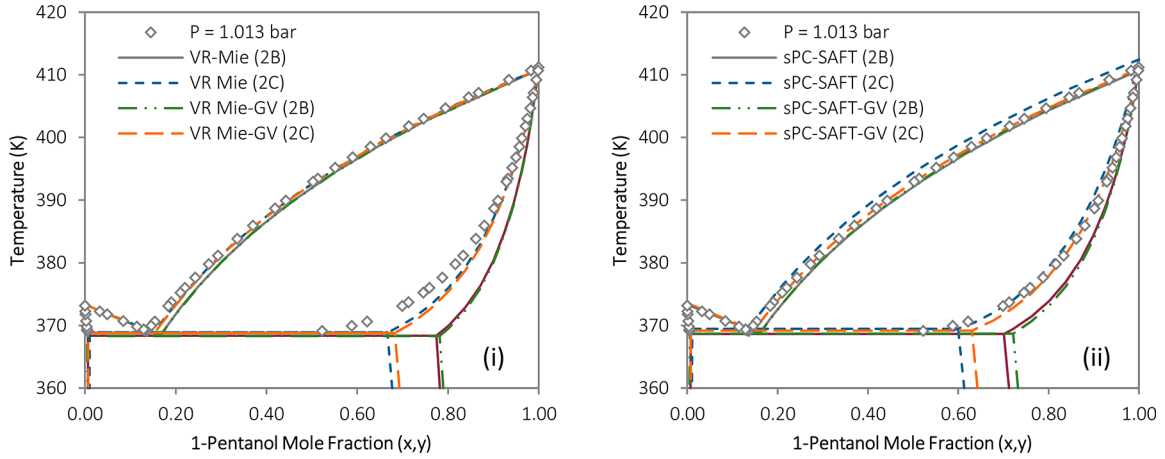

Figure 8. Comparison of predictions for polar and nonpolar models, considering the 2B and 2C schemes, applied to the 1-pentanol/water system at 1.013 bar:[82] (i) SAFT-VR Mie and (ii) sPC-SAFT with literature parameters.[7,27,48]

completely overpower the dipolar effects in the C_1-C_3 alcohols and that attempting to account for the influence of the molecular dipole is thus unnecessary: the magnitude of the regressed n_p values (viz. < 1) for these components support this conclusion.

Discerning between the performance of the 2B and 2C scheme parameter sets in Figure 5, the choice of association scheme does not appear to affect the predictions in the alcohol/*n*-alkane systems for both the polar and nonpolar models. The only notable difference in prediction quality between association schemes was for methanol, where application of the rigorous 3B scheme resulted in markedly poorer description of mixture behavior than either the 2B or 2C scheme equivalents, with only the 2C scheme correctly predicting a homogeneous equilibrium system. This is highlighted in Figure 6 for the methanol/*n*-hexane system, where false liquid splitting is predicted by both the 3B and 2B schemes. The poor prediction quality is emphasized by the fact that the specific dataset in question was incorporated in the objective function of the MD regressed parameters. These results strongly suggest that the rigorous treatment of the 3B scheme is not appropriate, even for the smallest alcohol in which three-site association is most physically feasible.

Achieving accurate VLE predictions for aqueous alcohol mixtures are notoriously difficult for equations of state, with SAFT-type models frequently resorting to correlation of these systems and the fitting of binary interaction parameters. With the focus on pure predictions in this work, the AADs for aqueous alcohol mixtures in Table 6 can be analyzed in the appropriate context. The overall prediction quality is comparable to the results of de Villiers et al.,[7,26] using the sPC-SAFT framework. This comparison is highlighted in Figure 7 for the 1-propanol/water system; this system provides a stringent test of the predictive capacity as 1-propanol is the largest linear alcohol that remains soluble in water at typical low-pressure VLE conditions, and accurate prediction of this homogeneity is difficult. For both SAFT variants, predictions based on the 2B scheme falsely predict VLLE behavior. In the case of sPC-SAFT, use of the 2C scheme resulted in the accurate prediction of a homogeneous liquid phase—this was not the case for the SAFT-VR Mie models, although a significant improvement in the prediction is still readily apparent using the 2C scheme. The sPC-SAFT and SAFT-VR Mie predictions for aqueous mixtures of the larger alcohols display much closer agreement, as Figure 8 shows for the 1-pentanol/water system. In this case, both models accurately capture the experimentally observed VLLE.

In comparing the different frameworks, it is interesting to note that, in the case of sPC-SAFT, the improved predictions for alcohol/water VLE using the 2C scheme coincided with

DOI: 10.1021/acs.iecr.8b01042
Ind. Eng. Chem. Res. 2018, 57, 9693−9706

decreased prediction quality for the alcohol/alkane systems using the same parameters.[7] As has already been highlighted in Figure 5 above, this is not the case for SAFT-VR Mie—the excellent predictions in evidence for both mixture types using a single parameter set and association scheme thus suggest a predictive robustness in the newer model. This result is reassuring, since the excellent VLE predictions for sPC-SAFT serve as a benchmark for assessing the performance of the new SAFT-VR Mie parameters applied to phase behavior both here and in our previous work.[23] While predictions of sPC-SAFT are explicitly optimized for phase behavior description, however, the promise of SAFT-VR Mie is in its ability to account for thermodynamic properties beyond phase behavior. We have already demonstrated the superiority of the variant in this regard in application to nonassociating components. The results presented here for alcohols will serve as the foundation for future work considering the prediction of non-VLE properties for associating components.

5. CONCLUSIONS

The objective of this work was to expand the practical application of the SAFT-VR Mie framework to consider alcohols and their mixtures in *n*-alkanes and water, respectively. New parameter sets for SAFT-VR Mie were determined to supplement or improve upon those presented in the original work, where the phase behavior of real fluid mixtures was not considered. In keeping with previous work done in our group, we further investigated the explicit consideration of dipolar effects by determining parameter sets for the polar SAFT-VR Mie-GV variant. In this way, full sets of parameters for all primary and secondary alcohols in the C_1−C_5 range, for both SAFT-VR Mie and SAFT-VR Mie-GV, were developed and presented.

The persistent problem of parameter degeneracy was once again evident in the parameter fitting, although novel use of the discretized regression approach allowed unique parameter sets to be determined for the affected components. The resulting parameter sets yield excellent predictions for pure component properties, with negligible difference in the performance of the polar and nonpolar models. The true test of the regressed parameter sets is in the prediction of mixture VLE, with alcohol/*n*-alkane and alcohol/water phase behavior considered. As with the pure-component properties, there was little to choose between the predictions of SAFT-VR Mie and SAFT-VR Mie-GV for these mixtures: the nonpolar model yielded better results for the smaller alcohols, while the polar variant was better suited to describing the behavior of longer chains ($\geq C_4$). The performance of these models was comparable for both primary and secondary alcohols, as well as for mixtures with *n*-alkanes and with water. Therefore, these results do not provide a definitive answer, regarding the role of an explicit polar term for associating components—certainly, the incorporation of an explicit polar term does not appear necessary for good phase equilibrium predictions to be attained. However, very notable differences in prediction accuracy were observed for different association schemes. The 2C scheme yielded comparable predictions to those of the 2B scheme for *n*-alkane mixtures, and a pronounced improvement in the description of aqueous mixtures. The more rigorous 3B scheme, which is considered only for methanol in this work, was found to be wholly unsuited to real fluid application.

With an emphasis on prediction quality in practical applications, the predictions of polar and nonpolar SAFT-VR Mie variants were compared to the benchmark performance of sPC-SAFT. The resulting predictions were of comparable quality, indicating that the regressed parameter sets represent a sound basis from which to conduct future work. Such work will look to consider different associating species and consider a wider range of thermodynamic properties.

AUTHOR INFORMATION

Corresponding Author

*E-mail: ajburger@sun.ac.za.

ORCID

Jamie T. Cripwell: 0000-0002-2439-5460

Cara E. Schwarz: 0000-0001-5513-2105

Notes

The authors declare no competing financial interest.

ACKNOWLEDGMENTS

The financial assistance of Sasol Technology (Pty) Ltd. and the Department of Trade and Industry (DTI) of South Africa through the Technology and Human Resources for Industry Programme (THRIP) toward this research is hereby acknowledged. The financial assistance of the Claude Leon Foundation and the National Research Foundation (NRF) of South Africa towards this research is hereby acknowledged. Opinions expressed and conclusions presented are those of the authors and are not necessarily to be attributed to the sponsors.

NOMENCLATURE

A^r = residual Helmholtz energy
A^{seg} = segment Helmholtz energy
A^{disp} = dispersion Helmholtz energy
A^{chain} = chain Helmholtz energy
$A^{assoc)}$ = association Helmholtz energy
d = temperature dependent segment diameter, Å
H^{vap} = heat of vaporization
k = Boltzmann constant, J K^{-1}
m = segment number
M_W = molecular weight, kg $kmol^{-1}$
n_p = number of polar segments
r_c^{AB} = range of association, Å
r_d^{AB} = distance between the associating site and its corresponding segment center, Å
P^{sat} = saturated vapor pressure, kPa
u^{liq} = speed of sound in compressed liquid phase, m s^{-1}
x_i = mole fraction
x_{pi} = fraction of dipolar segments
ε/k = dispersion energy parameter, K
ε^{AB}/k = association energy parameter, K
κ^{AB} = association volume
λ_a = Mie attractive range exponent
λ_r = Mie repulsive range exponent
μ = dipole moment, D
P^{liqt} = compressed liquid density, kg dm^{-3}
ρ^{sat} = saturated liquid density, kg dm^{-3}
σ = segment diameter, Å

Abbreviations

%AADz = percentage absolute average deviation in property z; %AADz = $100/n \sum_{i=1}^{n} |z_i^{cal} - z_i^{exp}|/z_i^{exp}$
AADz = absolute average deviation in property z, AADz = $1/n \sum_{i=1}^{n} |z_i^{cal} - z_i^{exp}|$
BIP(s) = binary interaction parameter(s)
EoS = equation of state

DOI: 10.1021/acs.iecr.8b01042
Ind. Eng. Chem. Res. 2018, 57, 9693−9706

FPP = fixed polar parameter (approach)
GC-SAFT = group contribution SAFT
(−)GV = Gross and Vrabec polar term (incorporated into the indicated framework)
JC = Jog and Chapman polar term
MD = mixture data (approach)
OF = objective function
PC-SAFT = perturbed chain SAFT
SAFT-VR = SAFT for potentials of variable range
SAFT-VR Mie = SAFT for Mie potentials of variable range
sPC-SAFT-GV = simplified PC-SAFT with GV polar term
SRP = standard regression procedure (approach)
TPT1 = thermodynamic perturbation theory of first order

REFERENCES

(1) Wertheim, M. S. Fluids with Highly Directional Attractive Forces. I. Statistical Thermodynamics. *J. Stat. Phys.* **1984**, *35* (1−2), 19−34.
(2) Wertheim, M. S. Fluids with Highly Directional Attractive Forces. II. Thermodynamic Perturbation Theory and Integral Equations. *J. Stat. Phys.* **1984**, *35* (1−2), 35−47.
(3) Wertheim, M. S. Fluids with Highly Directional Attractive Forces. III. Multiple Attraction Sites. *J. Stat. Phys.* **1986**, *42* (3−4), 459−476.
(4) Wertheim, M. S. Fluids with Highly Directional Attractive Forces. IV. Equilibrium Polymerization. *J. Stat. Phys.* **1986**, *42* (3−4), 477−492.
(5) Chapman, W. G.; Gubbins, K. E.; Jackson, G.; Radosz, M. New Reference Equation of State for Associating Liquids. *Ind. Eng. Chem. Res.* **1990**, *29* (303), 1709−1721.
(6) Huang, S. H.; Radosz, M. Equation of State for Small, Large, Polydisperse and Associating Molecules. *Ind. Eng. Chem. Res.* **1990**, *29*, 2284−2294.
(7) De Villiers, A. J.; Schwarz, C. E.; Burger, A. J. New Association Scheme for 1-Alcohols in Alcohol/Water Mixtures with sPC-SAFT: The 2C Association Scheme. *Ind. Eng. Chem. Res.* **2011**, *50*, 8711−8725.
(8) Lafitte, T.; Bessières, D.; Piñeiro, M. M.; Daridon, J. L. Simultaneous Estimation of Phase Behavior and Second-Derivative Properties Using the Statistical Associating Fluid Theory with Variable Range Approach. *J. Chem. Phys.* **2006**, *124* (2), 024509.
(9) Lafitte, T.; Piñeiro, M. M.; Daridon, J. L.; Bessières, D. A Comprehensive Description of Chemical Association Effects on Second Derivative Properties of Alcohols through a SAFT-VR Approach. *J. Phys. Chem. B* **2007**, *111* (13), 3447−3461.
(10) Lafitte, T.; Apostolakou, A.; Avendaño, C.; Galindo, A.; Adjiman, C. S.; Müller, E. A.; Jackson, G. Accurate Statistical Associating Fluid Theory for Chain Molecules Formed from Mie Segments. *J. Chem. Phys.* **2013**, *139* (15), 154504.
(11) Dufal, S.; Lafitte, T.; Galindo, A.; Jackson, G.; Haslam, A. J. Developing Intermolecular-Potential Models for Use with the SAFT-VR Mie Equation of State. *AIChE J.* **2015**, *61* (9), 2891−2912.
(12) Dufal, S.; Lafitte, T.; Haslam, A. J.; Galindo, A.; Clark, G. N. I.; Vega, C.; Jackson, G. The A in SAFT: Developing the Contribution of Association to the Helmholtz Free Energy within a Wertheim TPT1 Treatment of Generic Mie Fluids. *Mol. Phys.* **2015**, *113*, 948−984.
(13) Papaioannou, V.; Lafitte, T.; Avendaño, C.; Adjiman, C. S.; Jackson, G.; Müller, E. A.; Galindo, A. Group Contribution Methodology Based on the Statistical Associating Fluid Theory for Heteronuclear Molecules Formed from Mie Segments. *J. Chem. Phys.* **2014**, *140*, 054107.
(14) Dufal, S.; Papaioannou, V.; Sadeqzadeh, M.; Pogiatzis, T.; Chremos, A.; Adjiman, C. S.; Jackson, G.; Galindo, A. Prediction of Thermodynamic Properties and Phase Behavior of Fluids and Mixtures with the SAFT-γ Mie Group-Contribution Equation of State. *J. Chem. Eng. Data* **2014**, *59*, 3272−3288.
(15) Sadeqzadeh, M.; Papaioannou, V.; Dufal, S.; Adjiman, C. S.; Jackson, G.; Galindo, A. The Development of Unlike Induced Association-Site Models to Study the Phase Behaviour of Aqueous Mixtures Comprising Acetone, Alkanes and Alkyl Carboxylic Acids with the SAFT-G Mie Group Contribution Methodology. *Fluid Phase Equilib.* **2016**, *407*, 39−57.
(16) Hutacharoen, P.; Dufal, S.; Papaioannou, V.; Shanker, R. M.; Adjiman, C. S.; Jackson, G.; Galindo, A. Predicting the Solvation of Organic Compounds in Aqueous Environments: From Alkanes and Alcohols to Pharmaceuticals. *Ind. Eng. Chem. Res.* **2017**, *56*, 10856−10876.
(17) Jackson, G.; Chapman, W. G.; Gubbins, K. E. Phase Equilibria of Associating Fluids: Spherical Molecules with Multiple Bonding Sites. *Mol. Phys.* **1988**, *65* (1), 1−31.
(18) Müller, E. K.; Gubbins, K. E. An Equation of State for Water from a Simplified Intermolecular Potential. *Ind. Eng. Chem. Res.* **1995**, *34*, 3662−3673.
(19) Design Institute for Physical Properties of the American Institute of Chemical Engineers. *DIPPR 801 Database*; available via the Internet at: https://www.aiche.org/dippr/eventsproducts/%0A801-database.
(20) Sauer, S. G.; Chapman, W. G. A Parametric Study of Dipolar Chain Theory with Applications to Ketone Mixtures. *Ind. Eng. Chem. Res.* **2003**, *42* (22), 5687−5696.
(21) Jog, P. K.; Sauer, S. G.; Blaesing, J.; Chapman, W. G. Application of Dipolar Chain Theory to the Phase Behavior of Polar Fluids and Mixtures. *Ind. Eng. Chem. Res.* **2001**, *40* (21), 4641−4648.
(22) Gross, J.; Vrabec, J. An Equation-of-State Contribution for Polar Components: Dipolar Molecules. *AIChE J.* **2006**, *52* (3), 1194−1204.
(23) Cripwell, J. T.; Schwarz, C. E.; Burger, A. J. SAFT-VR-Mie with an Incorporated Polar Term for Accurate Holistic Prediction of the Thermodynamic Properties of Polar Components. *Fluid Phase Equilib.* **2018**, *455*, 24−42.
(24) Müller, E. K.; Gubbins, K. E. Molecular-Based Equations of State for Associating Fluids: A Review of SAFT and Related Approaches. *Ind. Eng. Chem. Res.* **2001**, *40*, 2193−2211.
(25) Al-Saifi, N. M.; Hamad, E. Z.; Englezos, P. Prediction of Vapor-Liquid Equilibrium in Water-Alcohol-Hydrocarbon Systems with the Dipolar Perturbed-Chain SAFT Equation of State. *Fluid Phase Equilib.* **2008**, *271* (1−2), 82−93.
(26) De Villiers, A. J.; Schwarz, C. E.; Chobanov, K. G.; Burger, A. J. Application of sPC-SAFT-JC and sPC-SAFT-GV to Phase Equilibria Predictions of Alkane/alcohol, Alcohol/alcohol, and Water/alcohol Binary Systems. *Ind. Eng. Chem. Res.* **2014**, *53* (14), 6065−6075.
(27) De Villiers, A. J.; Schwarz, C. E.; Burger, A. J. Improving Vapour-Liquid-Equilibria Predictions for Mixtures with Non-Associating Polar Components Using sPC-SAFT Extended with Two Dipolar Terms. *Fluid Phase Equilib.* **2011**, *305* (2), 174−184.
(28) Fouad, W. A.; Wang, L.; Haghmoradi, A.; Gupta, S. K.; Chapman, W. G. Understanding the Thermodynamics of Hydrogen Bonding in Alcohol-Containing Mixtures: Self Association. *J. Phys. Chem. B* **2015**, *119* (44), 14086−14101.
(29) Jog, P. K.; Chapman, W. G. Application of Wertheim's Thermodynamic Perturbation Theory to Dipolar Hard Sphere Chains. *Mol. Phys.* **1999**, *97* (3), 307−319.
(30) Karakatsani, E. K.; Spyriouni, T.; Economou, I. G. Extended Statistical Associating Fluid Theory (SAFT) Equations of State for Dipolar Fluids. *AIChE J.* **2005**, *51* (8), 2328−2342.
(31) Karakatsani, E. K.; Kontogeorgis, G. M.; Economou, I. G. Evaluation of the Truncated Perturbed Chain-Polar Statistical Associating Fluid Theory for Complex Mixture Fluid Phase Equilibria. *Ind. Eng. Chem. Res.* **2006**, *45*, 6063−6074.
(32) Linstrom, P.; Mallard, W. *NIST Chemistry Webbook*; NIST Standard Reference Database Number 69; available via the Internet at: http://webbook.nist.gov.
(33) Sun, T.; Biswas, S. N.; Trappeniers, N. J.; Ten Seldam, C. A. Acoustic and Thermodynamic Properties of Methanol from 273 to

DOI: 10.1021/acs.iecr.8b01042
Ind. Eng. Chem. Res. 2018, 57, 9693−9706

333 K and at Pressures to 280 MPa. *J. Chem. Eng. Data* **1988**, *33*, 395−398.
(34) Wegge, R.; Richter, M.; Span, R. Speed of Sound Measurements in Ethanol and Benzene over the Temperature Range from (253.2 to 353.2) K at Pressures up to 30 MPa. *J. Chem. Eng. Data* **2015**, *60*, 1345−1353.
(35) Dzida, M.; Ernst, S. Speed of Sound in Propan-1-ol + Heptane Mixtures under Elevated Pressures. *J. Chem. Eng. Data* **2003**, *48*, 1453−1457.
(36) Kumar, H.; Kaur, M.; Gaba, R.; Kaur, K. Thermodynamics of Binary Liquid Mixtures of Cyclopentane with 2-Propanol, 1-Butanol and 2-Butanol at Different Temperatures. *J. Therm. Anal. Calorim.* **2011**, *105*, 1071−1080.
(37) Dávila, M. J.; Gedanitz, H.; Span, R. Speed of Sound in Saturated Aliphatic Alcohols (Propan-2-ol, Butan-2-ol, and 2-Methylpropan-1-ol) and Alkanediols (Ethane-1,2-Diol, Propane-1,2- and -1,3-Diol) at Temperature between 253.15K and 353.15K and Pressures up to 30 MPa. *J. Chem. Thermodyn.* **2016**, *101*, 199−206.
(38) Wilson, W.; Bradley, D. Speed of Sound in Four Primary Alcohols as a Function of Temperature and Pressure. *J. Acoust. Soc. Am.* **1964**, *36* (2), 333−337.
(39) Papari, M. M.; Ghodrati, H.; Fadaei, F.; Sadeghi, R.; Behrouz, S.; Soltani Rad, M. N.; Moghadasi, J. Volumetric and Ultrasonic Study of Mixtures of 2-Phenylethanol with 1-Butanol, 2-Butanol, and 2-Methyl-1-Butanol at T = (298.15−323.15) K and Atmospheric Pressure: Measurement and Prediction. *J. Mol. Liq.* **2013**, *180*, 121−128.
(40) Khasanshin, T. S. Sonic Velocity in Liquid Primary Normal Alcohols. *Teplofiz. Vysok. Temp.* **1991**, *29*, 710−716.
(41) González-Salgado, D.; Troncoso, J.; Plantier, F.; Daridon, J. L.; Bessières, D. Study of the Volumetric Properties of Weakly Associated Alcohols by Means of High-Pressure Speed of Sound Measurements. *J. Chem. Thermodyn.* **2006**, *38*, 893−899.
(42) Dominik, A.; Chapman, W. G.; Kleiner, M.; Sadowski, G. Modeling of Polar Systems with the Perturbed-Chain SAFT Equation of State. Investigation of the Performance of Two Polar Terms. *Ind. Eng. Chem. Res.* **2005**, *44* (17), 6928−6938.
(43) Fouad, W. A.; Wang, L.; Haghmoradi, A.; Asthagiri, D.; Chapman, W. G. Understanding the Thermodynamics of Hydrogen Bonding in Alcohol-Containing Mixtures: Cross-Association. *J. Phys. Chem. B* **2016**, *120*, 3388−3402.
(44) Cripwell, J. T.; Schwarz, C. E.; Burger, A. J. Polar (s)PC-SAFT: Modelling of Polar Structural Isomers and Identification of the Systematic Nature of Regression Issues. *Fluid Phase Equilib.* **2017**, *449*, 156−166.
(45) Nguyen-Huynh, D.; Falaix, A.; Passarello, J.-P.; Tobaly, P.; de Hemptinne, J.-C. Predicting VLE of Heavy Esters and Their Mixtures Using GC-SAFT. *Fluid Phase Equilib.* **2008**, *264* (1), 184−200.
(46) Tumakaka, F.; Sadowski, G. Application of the Perturbed-Chain SAFT Equation of State to Polar Systems. *Fluid Phase Equilib.* **2004**, *217* (2), 233−239.
(47) Albers, K.; Heilig, M.; Sadowski, G. Reducing the Amount of PCP−SAFT Fitting Parameters. 2. Associating Components. *Fluid Phase Equilib.* **2012**, *326*, 31−44.
(48) Grenner, A.; Kontogeorgis, G. M.; von Solms, N.; Michelsen, M. L. Modeling Phase Equilibria of Alkanols with the Simplified PC-SAFT Equation of State and Generalized Pure Compound Parameters. *Fluid Phase Equilib.* **2007**, *258* (1), 83−94.
(49) Nath, A.; Bender, E. On the Thermodynamics of Associated Solutions. I. An Analytical Method for Determining the Enthalpy and Entropy of Association and Equilibrium Constant for Pure Liquid Substances. *Fluid Phase Equilib.* **1981**, *7*, 275−287.
(50) Clark, G. N. I.; Haslam, A. J.; Galindo, A.; Jackson, G. Developing Optimal Wertheim-like Models of Water for Use in Statistical Associating Fluid Theory (SAFT) and Related Approaches. *Mol. Phys.* **2006**, *104* (22−24), 3561−3581.
(51) Grenner, A.; Kontogeorgis, G. M.; Michelsen, M. L.; Folas, G. K. On the Estimation of Water Pure Compound Parameters in Association Theories. *Mol. Phys.* **2007**, *105* (13−14), 1797−1801.
(52) Dos Ramos, M. C.; Docherty, H.; Blas, F. J.; Galindo, A. Application of the Generalised SAFT-VR Approach for Long-Ranged Square-Well Potentials to Model the Phase Behaviour of Real Fluids. *Fluid Phase Equilib.* **2009**, *276*, 116−126.
(53) Gil-Villegas, A.; Galindo, A.; Whitehead, P. J.; Mills, S. J.; Jackson, G.; Burgess, A. N. Statistical Associating Fluid Theory for Chain Molecules with Attractive Potentials of Variable Range. *J. Chem. Phys.* **1997**, *106* (10), 4168−4186.
(54) Patel, B. H.; Docherty, H.; Varga, S.; Galindo, A.; Maitland, G. C. Generalized Equation of State for Square-Well Potentials of Variable Range. *Mol. Phys.* **2005**, *103* (1), 129−139.
(55) Katz, K.; Newman, M. Vapor−Liquid Equilibria for Ethyl Alcohol-*N*-Heptane at Low Pressure. *Ind. Eng. Chem.* **1956**, *48* (1), 137−141.
(56) Kontogeorgis, G. M.; Tsivintzelis, I.; Von Solms, N.; Grenner, A.; Bøgh, D.; Frost, M.; Knage-Rasmussen, A.; Economou, I. G. Use of Monomer Fraction Data in the Parametrization of Association Theories. *Fluid Phase Equilib.* **2010**, *296*, 219−229.
(57) Koh, C. A.; Tanaka, H.; Walsh, J. M.; Gubbins, K. E.; Zollweg, J. A. Thermodynamic and Structural Properties of Methanol- Water Mixtures: Experiment, Theory, and Molecular Simulation. *Fluid Phase Equilib.* **1993**, *83*, 51−58.
(58) Tybjerg, P. C. V.; Kontogeorgis, G. M.; Michelsen, M. L.; Stenby, E. H. Phase Equilibria Modeling of Methanol-Containing Systems with the CPA and sPC-SAFT Equations of State. *Fluid Phase Equilib.* **2010**, *288* (1), 128−138.
(59) Wolff, H.; Höppel, H.-E. Deuteriumbrückenassoziation U. Konzentrationsabhängiger Dampfdruck-Isotopie-Effekt von Methanol in *n*-Hexan. *Ber. Bunsen. Phys. Chem.* **1968**, *72* (6), 722−725.
(60) Pena, M. D.; Cheda, D. R. Liquid−Vapor Equilibrium. III. Systems of *n*-Propanol-*n*-Hexane at 50. Deg. and *n*-Propanol-*n*-Heptane at 60. Deg. *An. Quim.* **1970**, *66*, 747−755.
(61) Maciel, M. R.; Francesconi, A. Z. Excess Gibbs Free Energies of (*n*-Hexane + Propan-1-ol) at 338.15 and 348.15 K and of (*n*-Hexane + Propan-2-ol) at 323.15, 338.15 and 348.15 K. *J. Chem. Thermodyn.* **1988**, *20*, 539−544.
(62) Berro, C.; Péneloux, A. Excess Gibbs Energies and Excess Volumes of 1-Butanol-*n*-Heptane and 2-Methyl-1-Propanol-*n*-Heptane Binary Systems. *J. Chem. Eng. Data* **1984**, *29*, 206−210.
(63) Kumar, A.; Katti, S. S. Excess Free Energy of Binary Mixtures of Isomeric Butanols with Normal-Heptane. *Indian J. Chem., Sect. A: Inorg., Bio-inorg., Phys. Theor. Anal. Chem.* **1980**, *19*, 795−797.
(64) Máchová, I.; Linek, J.; Wichterle, I. Vapour−Liquid Equilibria in the Heptane−1-Pentanol and Heptane−3-Methyl-1-Butanol Systems at 75, 85 and 95 °C. *Fluid Phase Equilib.* **1988**, *41*, 257−267.
(65) Wolfová, J.; Linek, J.; Wichterle, I. Vapour—liquid Equilibria in the heptane−2-Pentanol and heptane−2-Methyl-1-Butanol Systems at 75, 85 and 95°C. *Fluid Phase Equilib.* **1991**, *64*, 281−289.
(66) Wolfová, J.; Linek, J.; Wichterle, I. Vapour−Liquid Equilibria in the Heptane−3-Pentanol and Heptane−2-Methyl-2-Butanol Systems at Constant Temperature. *Fluid Phase Equilib.* **1990**, *54*, 69−79.
(67) Oracz, P. Recommendations for VLE Data on Binary 1-Alkanol + *n*-Alkane Systems. *Fluid Phase Equilib.* **1993**, *89*, 103.
(68) Budantseva, L. S.; Lesteva, T. M.; Nemtsov, M. S. Liquid−Vapor Equilibrium in Systems Methanol−C7−8 Hydrocarbons of Different Classes. *Zh. Fiz. Khim.* **1975**, *49*, 1844.
(69) Pena, M. D.; Cheda, D. R. Liquid−Vapor Equilibrium. II. Ethanol-*n*-Heptane System at 40 and 60. Deg. *An. Quim.* **1970**, *66*, 737−745.
(70) Boublikova, L.; Lu, B. Isothermal Vapour−liquid Equilibria for the Ethanol−n-octane System. *J. Appl. Chem.* **1969**, *19* (3), 89−92.
(71) Hiaki, T.; Takahashi, K.; Tsuji, T.; Hongo, M.; Kojima, K. Vapor−Liquid Equilibria of Ethanol + Octane at 343.15 K and 1-Propanol + Octane at 358.15 K. *J. Chem. Eng. Data* **1995**, *40*, 271−273.
(72) Heintz, A.; Dolch, E.; Lichtenthaler, R. N. New Experimental VLE-Data for Alkanol/alkane Mixtures and Their Description by an Extended Real Association (ERAS) Model. *Fluid Phase Equilib.* **1986**, *27*, 61−79.

DOI: 10.1021/acs.iecr.8b01042
Ind. Eng. Chem. Res. 2018, 57, 9693−9706

(73) Araujo, M. E.; Maciel, M. R. W.; Francesconi, A. Z. Excess Gibbs Free Energies of (Hexane + Butan-2-ol) and of (Cyclohexane + Butan-2-ol) at the Temperatures (323.15, 338.15, and 348.15) K. *J. Chem. Thermodyn.* **1993**, *25*, 1295−1299.
(74) Ronc, M.; Ratcliff, G. R. Measurement of Vapor-liquid Equilibria Using a Semi-continuous Total Pressure Static Equilibrium Still. *Can. J. Chem. Eng.* **1976**, *54* (4), 326−332.
(75) Kurihara, K.; Minoura, T.; Takeda, K.; Kojima, K. Isothermal Vapor−Liquid Equilibria for Methanol + Ethanol + Water, Methanol + Water, and Ethanol + Water. *J. Chem. Eng. Data* **1995**, *40*, 679−684.
(76) Kojima, K.; Tochigi, K.; Seki, H.; Watase, K. Determination of Vapor-Liquid Equilibrium from Boiling Point Curve. *Kagaku Kogaku* **1968**, *32*, 149−153.
(77) Danner, R. P.; Gess, M. A. A Data Base Standard for the Evaluation of Vapor−Liquid-Equilibrium Models. *Fluid Phase Equilib.* **1990**, *56*, 285−301.
(78) Woerpel, U.; Vohland, P.; Schuberth, H. The Effect of Urea on the Vapor−Liquid Equilibrium Behavior of *n*-Propanol/water at 60 C. *Z. Phys. Chem.* **1977**, *258* (5), 905.
(79) Gabaldón, C.; Marzal, P.; Montón, J. B.; Rodrigo, M. A. Isobaric Vapor−Liquid Equilibria of the Water + 1-Propanol System at 30, 60, and 100 kPa. *J. Chem. Eng. Data* **1996**, *41*, 1176−1180.
(80) Arce, A.; Arce, A., Jr; Martínez-Ageitos, J.; Rodil, E.; Soto, A. (Vapour + Liquid) Equilibrium of (DIPE + IPA + Water) at 101.32 kPa. *J. Chem. Thermodyn.* **2003**, *35*, 871−884.
(81) Lladosa, E.; Montón, J. B.; Cruz Burguet, M.; Muñoz, R. Phase Equilibrium for the Esterification Reaction of Acetic Acid + Butan-1-ol at 101.3 kPa. *J. Chem. Eng. Data* **2008**, *53*, 108−115.
(82) Iwakabe, K.; Kosuge, H. Isobaric Vapor−liquid−liquid Equilibria with a Newly Developed Still. *Fluid Phase Equilib.* **2001**, *192*, 171−186.

DOI: 10.1021/acs.iecr.8b01042
Ind. Eng. Chem. Res. 2018, 57, 9693−9706